Thickness Influence On The Synthesis Of Metal Oxide NiO Using RF- Magnetron Sputtering

Ehssan Salah Hassan , Mohammed Hadi Salih, Ahmed N. Abd
Department of physics, college of science, Al-Mustansiriyah Univ. Baghdad, Iraq
Ministry of Science and Technology, department of applied physics Baghdad, Iraq
Department of physics, college of science, Al-Mustansiriyah Univ. Baghdad, Iraq
ahmed_naji_abd@yaho.com

Abstract—These work studies dependences of structural properties, mobility and charge carrier concentration on the thickness of nickel oxide (NiO) nano films deposited on glass substrates by RF reactive magnetron sputtering at an RF power 200 W. The X-ray diffraction (XRD) analyses of nickel oxide nano films indicates that these films are polycrystalline with preferred orientation along (200) plane, crystallite sizes increased from 22.894 nm, to 25.035 nm when the film thickness increase from 50 nm to 150 nm. The microstrain (ε) and dislocation density (δ) decrease as the thickness increases. The average roughness increased from 2.055 nm to 3.191 nm as the thickness increasing. The resistivity of NiO film is increased with an increase in film thickness, which is related to the decrease of carrier concentration with film thickness. The NiO film with a thickness of 150 nm has a maximum resistivity of 50.92 KΩ.cm

Keywords—Nickel oxide films; reactive Sputtering; XRD; Structure; Electrical properties

1-Introduction

Nickel oxide (NiO) is the most exhaustively investigated transitional Matel oxide. It is a NaCl P-type antiferromagnetic oxide semiconductor. It offers promising candidature for many applications such as solar thermal absorber [1], catalyst for O_2 evolution [2], photo electrolysis [3], electrochromic device [4], and functional sensor layers for chemical sensors [5] These films have been fabricated using various physical and chemical vapor deposition techniques such as thermal oxidation of nickel [6], chemical bath deposition [7], spray pyrolysis [8], sol-gel process [9], electron beam evaporation [10], atomic layer deposition [11], pulsed laser deposition [12], metal organic chemical vapor deposition [13], molecular beam epitaxial [14], and DC [15] and RF magnetron sputtering and electro deposition [16], Among these methods, reactive sputtering is the most extensively used. Researches [17] have been carried out on the dependence of film properties on sputtering parameters. Numerous reference data and previous studies [18] Have demonstrated that superior electric and optical properties of NiO films can be obtained by reactive sputtering with a sputtering pressure in the range 0.1–1 Pa and in a pure oxygen atmosphere using a heated substrate. The increase in surface area and the quantum confinement effects have made nanostructured materials are quite distinct from their bulk form in both electrical and optical properties various one-dimensional structures of NiO, such as nanowires, nanorods, and Nano belts, have attracted much attention [19]. Among these deposition techniques, magnetron sputtering is industrially adopted thin films preparation method because of the advantages in the generation of uniform and large area films. The physical properties of the sputtering films depends mainly on the process parameters such as oxygen partial pressure, sputter power, substrate temperature, substrate bias, thickness and post deposition annealing The influences of film thickness on the structural, optical, and electrical properties of thin films are very important. Many reports on the effect of size on thin films of various materials have been published. [20] However, only few works on the dependence of the properties nickel oxide films on film thickness have been published [21].

2-Experimental

Thin films of nickel oxide were formed on to well cleaned glass substrates (Supe Rior w. Germany) held at temperature range 40oC – 50oC which is the sputter chamber temperature by RF magnetron sputtering method. Metallic nickel target (99.99 % pure supplied by Nuclear Fuel Complex, India) with 50 mm diameter and 3mm thickness was used as sputter target for deposition of the films in the sputter dawn configuration. The deposition rate kept at (0.1 – 0.2) Å/sec by the deposition rate and thickness controlled by crystal sensor (FTM-2000). The distance between target and the substrate was (100 mm). The sputter chamber was evacuated to the base pressure of $4.1x10^{-6}$ torr employing molecular devotion and turbo combination. Pressure in the sputter chamber was measured with digital Pirani - Penning gauge (adixen ACS 2000) combination. Argon and oxygen (99.999 % purity) were used as sputter and reactive gases for deposition of the films. Individual Argon and Oxygen gases penetrate to

the chamber with gas mass flue controller (Ailcat scientific) controllers were employed to admit these gases in required quantities in the sputter chamber. Argon gas was introduced to the pressure of $8.68x10^{-3}$ torr. Later Oxygen gas was admitted with pressure of $5.18x10^{-2}$ torr. Radio frequency (13.5 KHz) RF power (TORR INTERNATIONAL, INC.CRC600) used to feed the sputter target of 200

W. The crystal structure of deposited films was identified by the X-ray diffraction (XRD) (shimadzo 6-2000, with cuk_{α} radiation having wavelength λ=0.15406 nm) technique. The surface microstructure was studded by (S-4160) Hitachi (college of engineering and communications, iran-tahran) scanning electron microscopy (SEM), the surface roughness was studded by (SPM AA 3000, contact mode, angstrom advanced INC.) atomic force microscopy (AFM). The Hall measurements, resistivity, mobility and carrier concentration of the films were measured by using an (Digital multi meter: The PC –interfaced multi meter, of type Proskit (MT-1820).angstrom).

3- *Result and discussion*

Film thickness is one of the critical factors for application of transparent and the gases sensors films. NiO films with different thicknesses were controlled by the crystal sensor at fixed deposition rate around (0.1- 0.2 Å\sec) and by fixing other deposition parameters as constant. Fig. (1) Shows the X-ray diffraction profiles of NiO films in the thickness of (50, 100, and150) nm. From the XRD profile, all the films were polycrystalline nature [22] consisting nickel oxide cubic phase with sharp and very fine peaks indicate a good crystallization and the major peak is along (200) plane at 2 θ (42.98 º), This is for cubic crystal structure under the space group Fm3m with high intensity indicate the dominate growth direction according to ASTM card [No.00-047-1049] [23]. Minor small peaks along (111) and (220) planes corresponding to the angels 2θ = 37.23º and 2θ = 62.34º respectively for thickness 50 nm, and only (111) reflection for both thickness 100 nm and 150 nm. it is well known that the (200) plan of ionic rook salt materials is considered as non-polar cleavage plane and is thermodynamically stable, and the most stable NiO termination has the surface energy of 10.86×10^{18} $eV.m^{-2}$ with high intensity indicated that the Nano crystals were embedded in single crystalline matrix. As the film thickness increased to 100 nm, the intensity of the (200) was increased greatly indicated that increasing in the films crystallinitiy and the crystalline size increases from (22.894 nm to 24.438 nm) as the thickness increases from 50 nm to 100 nm and as shown in fig.(2-a). Further increase of

thickness to 150 nm the intensity of the diffraction peaks increases. Revealed the enhancement in the crystalinity of the films and the crystalline size increases to (25.036 nm). The peak intensity and crystalinity are associated with the crystalinity of the deposited films. According to the crystal growth mechanism the growth faces of crystallites correspond to the crystal shape of equilibrium determined by the orientation of the crystal [24]. The crystalline size of the films was calculated from the X-ray diffraction (200) reflection using the Debye- Scherer's relation (1) [25]**.**

$$L = \frac{K\lambda}{\beta cos\theta} \; (nm) \qquad\qquad (1)$$

Where β is the measured FWHM (in radiant), θ is the Bragg angel of the peak, the λ is the X-ray diffraction wavelength, L is the effective crystalline size. Dislocation density and microstrain developed on the thickness of the films and table (1) displays XRD data for NiO nano films deposited by RF reactive magnetron sputter.

Fig. (2-b) Shows the microstrain in the films that evaluated using the formula (2). The microstrain first decreased from 15.15×10^{-5} $line^{-2}.m^{-4}$ to 14.19×10^{-4} $line^{-2}.m^{-4}$ with increase of film thickness from(50 to 100) nm due to the enhancement in the crystalinity. A farther decrease in the microstrain to 13.85×10^{-4} $line^{-2}.m^{-4}$ at higher thickness of 150 nm was due to the increase in the crystalinity of the films and so the microstrain reduction is caused by varying displacements of the atoms with respect to their reference lattice position. [26].

$$\varepsilon = \frac{\beta cos\theta}{4} \; (lines^{-2}.m^{-4}) \; . \qquad (2)$$

Fig. (2-c) Shows the dislocation density (δ) defined as the length of the dislocation lines per unit volume of the crystal, evaluated using the formula (3) [27]. The dislocation density (δ) of the NiO films decreased from 1.90×10^{15} $lines/m^2$ to 1.67×10^{15} $lines.m^{-2}$ with increase of film thickness from 50 to 100 nm, there after increased to 1.59×10^{15} $lines.M^{-2}$ at higher thickness of 150 nm [28].

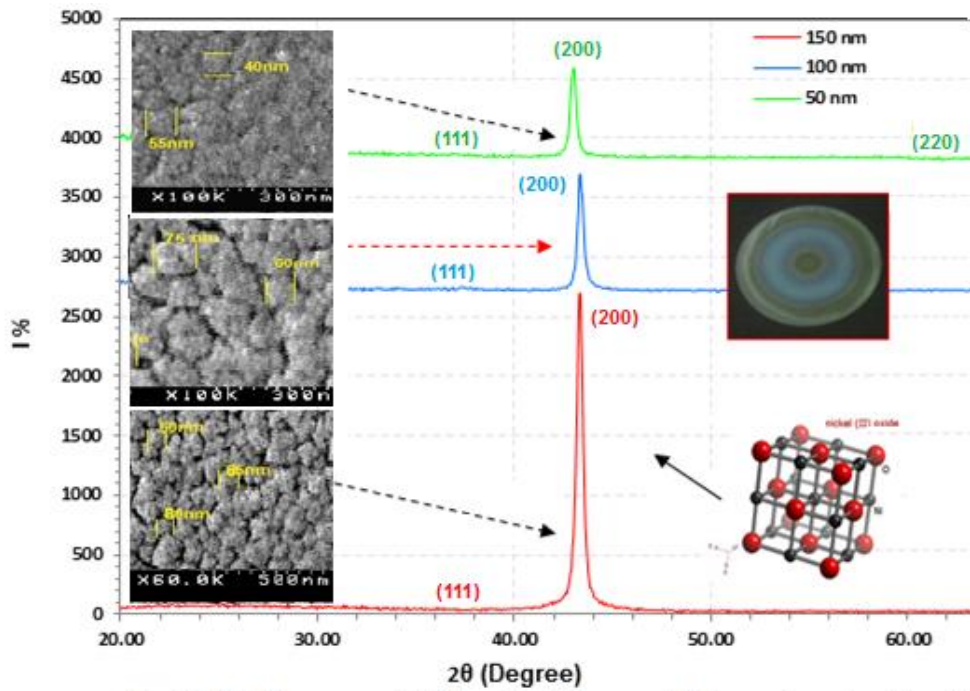$$\delta = \frac{n}{L^2} \; (line.m^2). \qquad\qquad (3)$$

fig.(1):XRD pattren of NiO with different thickness depoeited by rf-reactive magnetron sputter

Fig. (2-d) Shows the variation of full width at half maximum with the thickness of NiO films. The full width at half maximum intensity decreased from (0.37 to 0.35) with the increase of film thickness from 50 nm to 100 nm, thereafter it decreased to (0.34) at higher thickness of 150 nm. At low thickness of 50 nm the high value of full width at half maximum and small crystallite size of 24.894 nm was due to the single crystalline nature of the films and enhancement in the crystallite size.
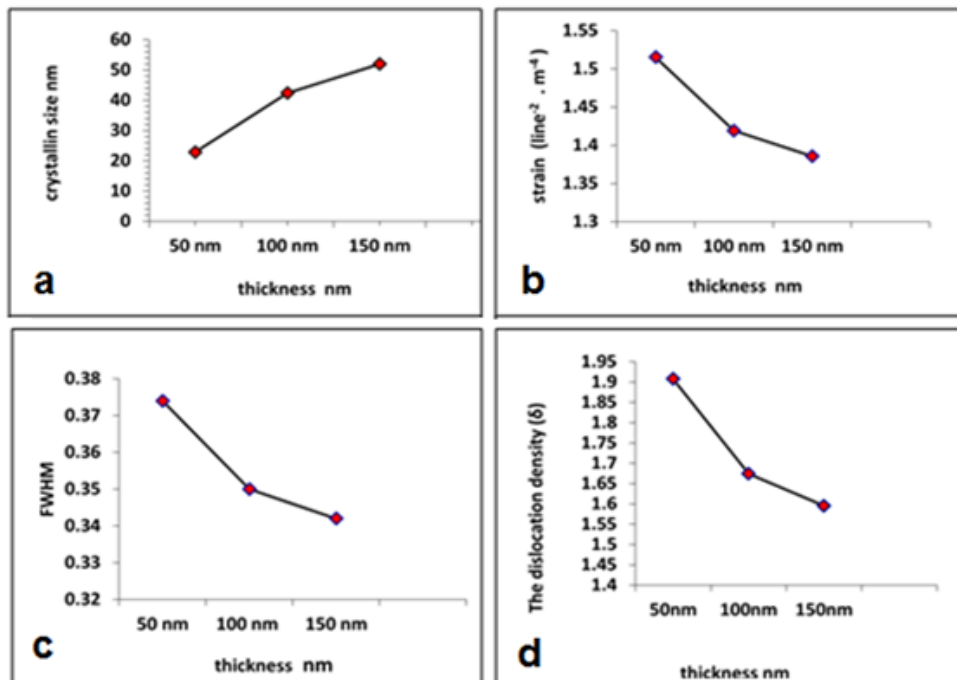

Fig.(2)(a) thickness Vs. crystalline size, (b) thickness Vs. microstrain , (c) thickness Vs. dislocation density, (d) thickness Vs. FWHM.

Table (1):Displays XRD data for NiO nano films deposited by RF reactive sputtering.

Thickness (nm)	(hkl)	FWHM	2θ(deg.)		d(A°)		D L (nm)	a (nm)
			XRD	ASTM	XRD	ASTM		
50	(200)	0.374	43.31	43.27	0.2087	0.2089	22.894	0.4174
100	(200)	0.350	42.98	43.27	0.2102	0.2089	24.438	0.4204
150	(200)	0.342	43.35	43.27	0.2085	0.2089	25.036	0.4170

Fig. (3) Shows the SEM images of NiO films of different thicknesses. It is seen from the figures that thin films of (3-a) 50 nm exhibited smaller grain size and compact surface with average grain size (60 nm). When the thickness of the films increased to 100 nm, fig.(3-b) the shape of nanorood presence of dense surface with porous like structure due to improvement in the crystallinity and increases in the average grain size to (70 nm) of the films . It was also supported by the XRD analysis that the crystallinity enhanced as the thickness of the films increased to 100 nm. Further increase of film thickness to 150 nm fig. (3-c), the porous surface structure improves and growth of nanorods with length of about 1300 nm. The increase of film thickness to 150 nm the average grain size increases to (75 nm) due to perfection in the crystallinity [29].
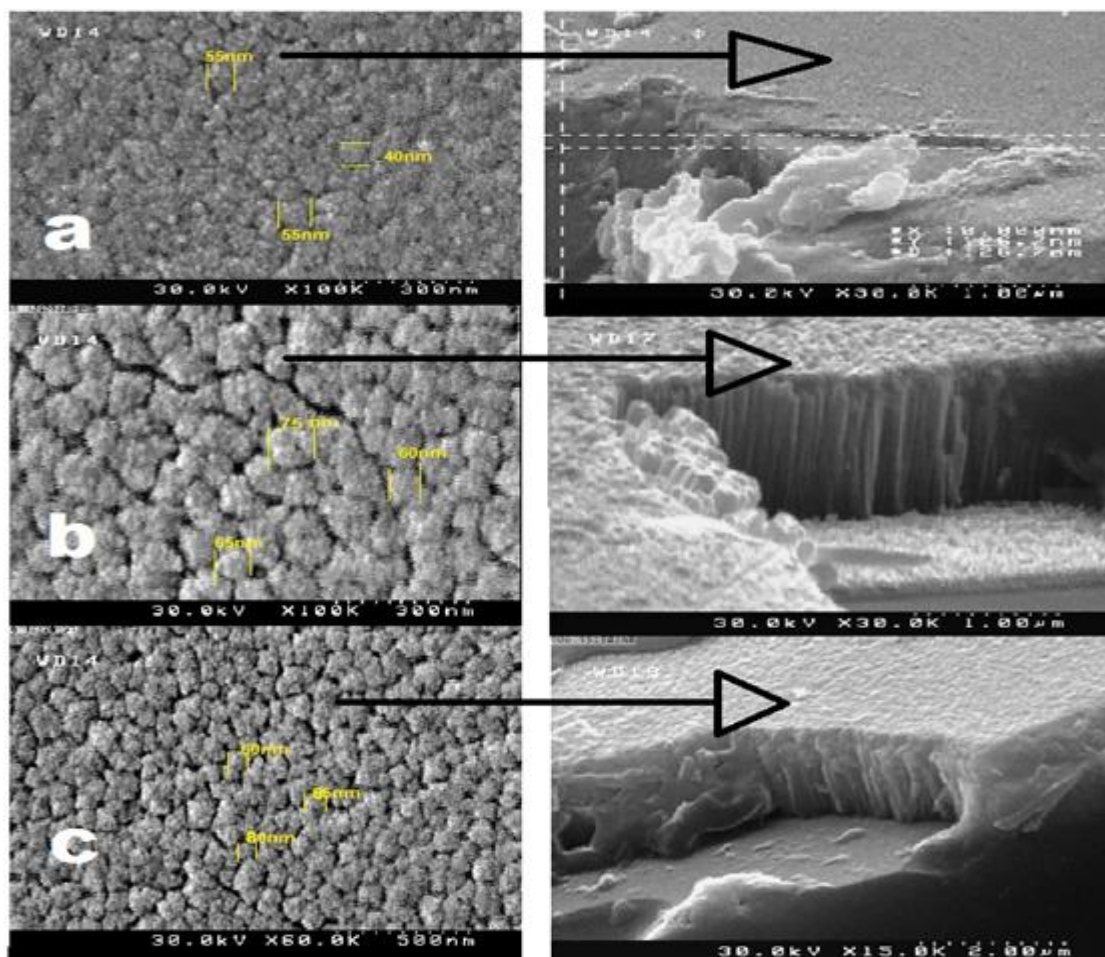

Fig.(3): SEM image top and cross section view (a) 50 nm (b)100 nm (c) 150 nm of NiO films deposited by RF reactive sputtering.

Fig (4). The atomic force microscopy was used to determine the root mean square roughness (RMS), roughness average and average grins size listed in the table (2). Figure (4-a) shows NiO of 50 nm thickness, root mean square (RMS), roughness average, and average grins size was (2.751, 2.055 and 42.6) nm respectively. With increase of film thickness to 150 nm as showmen in figure (4-c) the

root mean square (RMS), roughness average, and average grins size is, gradually increased to (4.012, 3.191 and 44.9) nm respectively. The increase of RMS roughness with the increase of film thickness was due to the larger size grains formation as well as increase in the porosity of the films [30].

Such an increase of film thickness was also noticed by Hoon et al. [31]. The increase of RMS roughness of NiO films leads significant effect on the industrial applications such as gas sensors Estimated from AFM, are given in Table(2).
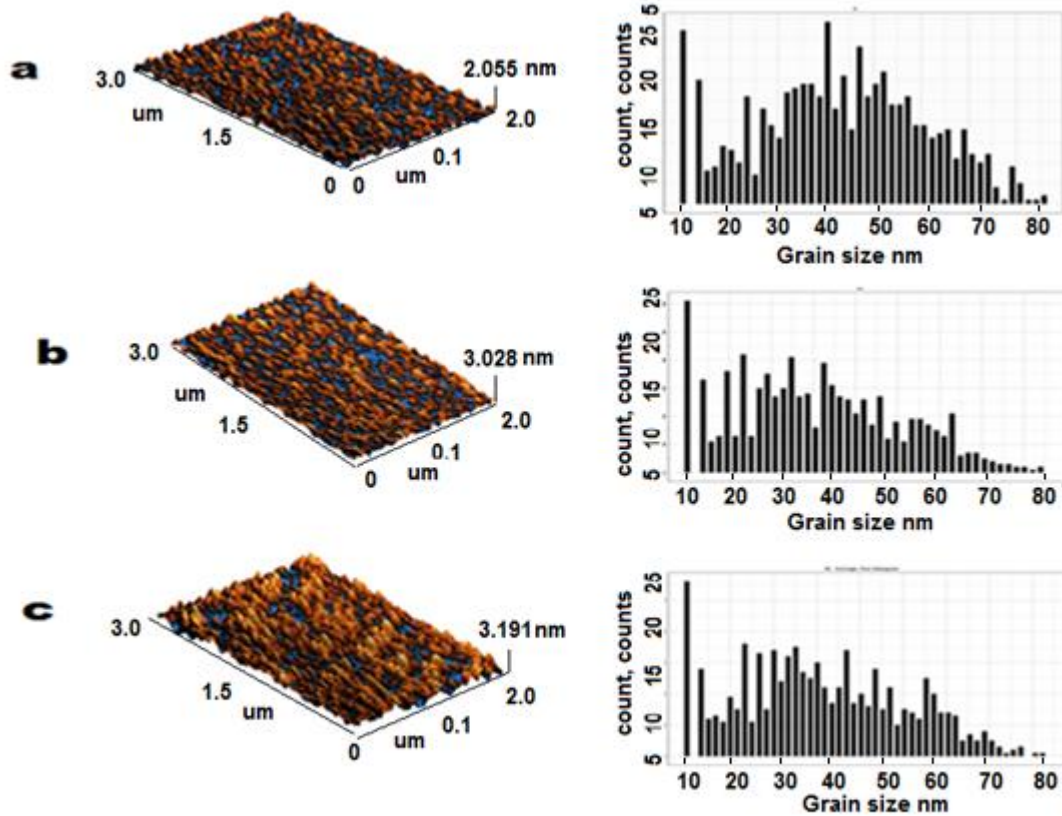

Fig.(4): AFM image of (a) 50 nm (b) 100 nm (c) 150 nm of NiO films deposited by RF reactive sputtering

Table (2): Grain size, roughness average, RMS of NiO nano films deposited by RF reactive sputtering

Thickness(nm)	Grain average size(nm)	RMS(nm)	Roughness Average(nm)
50	42.6	2.751	2.055
100	42.8	3.796	3.028
150	44.9	4.012	3.191

Fig (5) shows the Hall measurement for the NiO films with different thickness. We can see that all carrier concentrations (n_p) are positive for all NiO in the NiO composite films exhibit p-type conduction the

dependence of resistivity (ρ) and carrier concentration (n_p) on the thickness of the NiO films that were deposited by RF sputtering on substrate at different thickness. Figure (5-a,b) shows the resistivity and

carrier concentration of the NiO films. The resistivity fig.(5-a) is seen to increase from 4.0864×10^4 Ω.cm to 5.092×10^4 Ω.cm as the film thickness is increased from 50 to 150 nm. While the carrier concentration fig.(5-b) is seen to decrease from 6.067×10^6 cm^{-3} to 2.305×10^6 cm^{-3} as the film thickness is increased from 50 to 150 nm. The high resistivity of the deposited NiO nano films can be attributed relatively low mobility and high resistivity of the NiO thin film grown in high thickness originated from the high crystallinity and perfectly coinciding grain boundaries between the NiO clusters Imperfections and\or defects in thin films not

only works as trap sites but caused band stalking, and these bands combine with the nearest parent bands [32]. Therefor the resistivity increased as a result of the reduced extended states with decreasing imperfections. In addition the inversely relation between the resistivity and the carrier concentration is observed in relation (4).

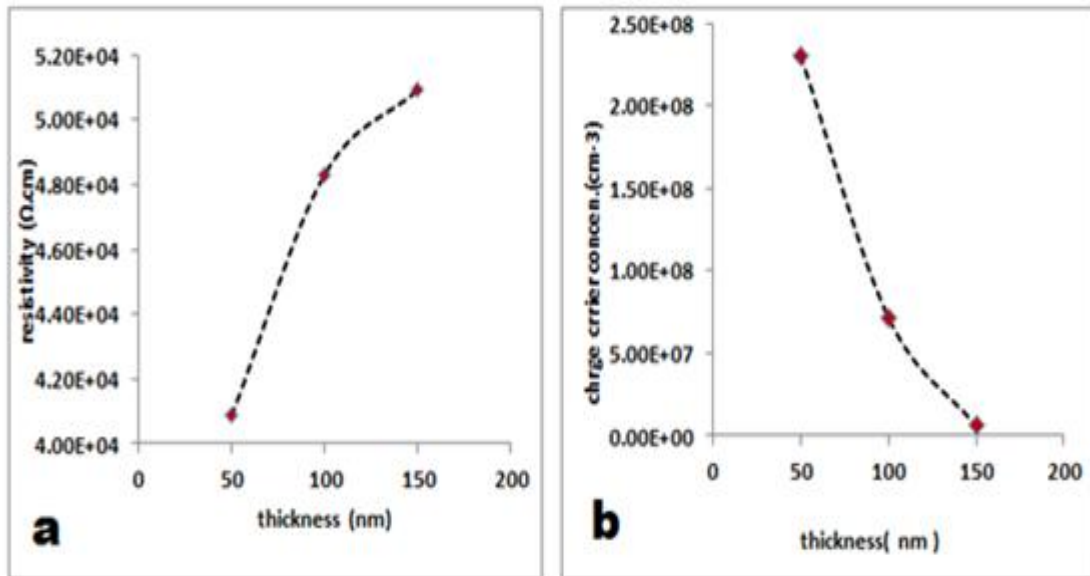$$\rho = \frac{1}{ne\mu} \ (4)$$

Where e is the electric charge .

Fig.(5): Hall measurements (a) resistivity Vs. thickness (b) charge carrier concentration Vs. thickness.

Conclusions

NiO thin films deposited by RF. Reactive magnetron sputter controlled by very fine deposing rate (0.1 – 0.2) Å/sec. can shows single crystalline structure. Structural properties strongly effect by thickness variation. The crystalline size increase as the film thickness increase, microstrain, dislocation density, FWHM decrease as

the film thickness increase .the surface morphology also effect by the variation of thickness and the surface becomes more rougher and not compact and nanorood structure growth can be observed as the thickness increases also (RMS), roughness average and average grain size increases as the film thickness increases. The electrical properties effected also by the varying the thickness .

References

[1]. E.Fujii, A.Tomozawa, H.torii and Takayama: japan.j.appl.35 (1996) 328-330.

[2]. K. Youshmura, T. Miki, S. Tanemura (nickel oxide electro-chromic thin films prepared by reactive

DC magnetron Sputtering jap.j. Appl. phys. 34, (1995), 2440- 2446.

[3]. M. Kitao, K.Izawa, K.Urabe, T.Komatso, S. Knwano and S.Yamada: Jap. Appl . phy.33 (1994) 6656-6662.

[4]. R.Tsu, L.Esaki, R, Ludeke, physic. Rev.23 (1996) -763.

[5]. M.Elahi, N.Ghobadi Iranian physic j, (2008). 26-30.

[6].P.pramank, S.Bhattachraga, J. Electrochemecal.soc. 137(1990) 3869.

[7]. L.D.Kadam, C.H.Bhosal, P.S.Patil, Tr.j.phy.21 (1997)1037.

[8]. D.Adler, L.H.Tejeng, F.C.Vooget, T.Hibma, G.A.J.vogel, phys .57 ,(1998) 11623.

[9]. Mario birkhols (thin film analysis by X-ray scattering) (2006) willey.vhc.

[10]. H.W.Ryu, G.P.Choi, W.S.Lee and s.park:j.mater sci.lett.39 (2004) .4375-4377.

[11]. B.D.Cuttity and S.R.stock, Element of X-ray diffraction, 3rd Ed. (2001).

[12]. S.sathyamurthy, R.senthilarasn, Lolitha, soler energy mater, solar Cell. (2004) 182-187.

[13]. N.Lee, Sh.Kim, Kakani, thin solid films. 2010. 494- 519.

[14]. A. J. Varkey and A. F. Fort, Solution growth technique for Deposition of nickel

oxide thin films, Thin Solid Films, vol. 235, No. 1-2. 1993. 47-50.

[15]. J. S. E. M. Svensson and C. G. Granqvist, Electrochromic Hydrated nickel oxide Coatings for energy efficient windows: Optical properties and coloration Mechanism, Applied Physics Letters, vol. 49, no. 23, 1566.

[16]. S. Yamada, T. Yoshioka, M. Miyashita, K. Urabe, andM. Kitao, Electrochromic Properties of sputtered nickel-oxide films, Journal of Applied Physics, vol. 63, No. 6, 1988. 2116–2119,.

[17]. M. boscarino, Ferroni, D. comini, E. gnani, V. guidi, V. martielli, G. nellii, P.rigato, V.sberveglieri, G,: Sensors and actuators B 58 (1999). 289

[18]. K.M. Dooley, S.Y. Chen, J.R.H. Ross, J. Catal. 145, 402 (1994) .

[19]. A. Iida and R. Nishikawa, A thin film of an Ni-NiO heterogen- Eoussystem for an optical recording medium, Japanese Journal of Applied Physics, vol. 33. 1994. 3952–3959.

[20]. E. Fujii, A. Tomozawa, H. Torii and R. Takayama: Jpn. J. Appl.

Phys. 35 (1996) .328–330

[21]. S. Y. Wang, Wei Wang, W. Z. Wang and Y. W. Du: Mater. Sci.

Eng. 90 (2002) 133–137.

[22] L.V.Azaroof." Elements of x-ray crystallography" Mc Graw-Hill book company (1968).

[23] Dott.Delia Puzzovio " Surface interaction mechanisms in metal-oxide semiconductors for alkane detection " a thesis in Universita degli studi di ferrara, 2008.

[24]. A. Sreedhar, M. Hari Prasad Reddy, S. Uthanna and J.F. Pierson,Sputter power influenced structural, electrical, and optical behaviour

Of nanocrystalline CuNiO2 films formed by RF magnetron

Sputtering , ISRN Cond. Matter Phys., 2013, Article ID 527341.

[25].M. Alagar, T. Theivasanthi and A. Kubera Raja, J. of App. Sci,

(2012). 12, 398.

[26]. T. Theivasanthi and M.Alagar, Nano Biomed. Eng. 3. (2011). 163.

[27]. J. G. Van Berkum , J. G. M. , A. C. Varmcuch , R. Delhen , Th. H.

Dinkeijser and E. J. Hemeijer. J. Appl. Crys. 27. (1994). 345-357.

[28]. T. Obata, K. Komeda, T. Nakao, H. Ueba, and C. Tasygama. J. Appl. Phys. (1997).81, 199.

[29]. U. Pal, D. Samanta, S. Ghoral, B. K. Samantaray and A. K. Chaudhuri: J. Phys. D: Appl. Phys. 25 (1992) 1488–1494.

[30]. L.D. Kadam, C.H. Bhosale, P.S. Patil, Tr. J. Phys. 21 (1997).

[31]. Hoon, JW; Chan, KY.; Krishnasamy, J.; Tou, TY. Knipp, D.

Appl. Surf. Sci. 2011, 257- 258

[32]. K. Oka; T. Yanagida; K. Nagashima,; H. Tanaka,; T. Kawai, . Appl.phys. 2008, 104, 013711.